Growth and optical properties of Dy^{3+}/Eu^{3+} co-doped $NaYF_4$ single crystals with cubic lattice for white LED application*

JIANG Dong-sheng (江东升)[1], **JIANG Yong-zhang** (姜永章)[1], **XIA Hai-ping** (夏海平)[1]**, **ZHANG Jia-zhong** (张加忠)[1], **YANG Shuo** (杨硕)[1], **GU Xue-mei** (谷雪梅)[1], **JIANG Hao-chuan** (江浩川)[2], **and CHEN Bao-jiu** (陈宝玖)[3]

1. Key Laboratory of Photoelectronic Materials, Ningbo University, Ningbo 315211, China

2. Ningbo Institute of Materials Technology and Engineering, Chinese Academy of Sciences, Ningbo 315211, China

3. Department of Physics, Dalian Maritime University, Dalian 116026, China

(Received 24 June 2015)

Dy^{3+}/Eu^{3+} co-doped cubic lattice $NaYF_4$ single crystal with high quality in the size of ~Φ1.0 cm×10.0 cm was grown by an improved Bridgman method using potassium fluoride (KF) as assistant flux. X-ray diffraction (XRD), absorption spectra, excitation spectra and emission spectra are measured to investigate the phase and luminescent properties of the crystal. The effects of excitation wavelength and concentrations of Dy^{3+} and Eu^{3+} ions on the luminescent characteristics are analyzed. The $NaYF_4$ single crystal with the doping molar concentrations of 1.205% Dy^{3+} and 0.366% Eu^{3+} exhibits an excellent white light emission with chromaticity coordinates of x=0.321, y=0.332. It indicates that the Dy^{3+}/Eu^{3+} co-doped cubic lattice $NaYF_4$ single crystal can be a potential luminescent material for the ultraviolet (UV) light excited white light emitting diode (w-LED).

Document code: A **Article ID:** 1673-1905(2015)05-0356-5

DOI 10.1007/s11801-015-5115-x

Transparent rare earth ion doped glasses[1] and single crystals[2,3] have recently become interesting as the single-phased full-color emitting solid state materials[4,5] for generating a white-light emission due to their unique properties, such as high resistance, low light scattering and low power consumption. However, there are few reports on rare earth ion doped single crystals for white light emitting diode (w-LED) due to the high cost of equipment and the technical difficulty in crystal growth[5]. More recently, Tm^{3+}/Dy^{3+}, Tb^{3+}/Sm^{3+} co-doped $LiYF_4$ single crystals were grown and the white light emissions were obtained in our laboratory[4]. It is known that the phonon energy of $NaYF_4$ (~360 cm^{-1})[6] is much lower than that of $LiYF_4$ (~ 650 cm^{-1})[7]. Generally, the quantum efficiency of rare earth ion is increased as the decrease of the phonon energy of host. Therefore, $NaYF_4$ is much promising and is of particular interest to be a host for rare earth ions. However, $NaYF_4$ single crystal is extremely hard to grow due to the complex phase equilibrium in NaF-YF_3 system. Up to now, there is no report about Dy^{3+}/Eu^{3+} co-doped $NaYF_4$ single crystal for w-LED application.

In this paper, the Dy^{3+} and Eu^{3+}co-doped cubic lattice $NaYF_4$ single crystal with big size was grown successfully from NaF-YF_3 system by an improved Bridgman method using potassium fluoride (KF) as assistant flux, and the technical growing parameters are optimized. The $NaYF_4$ in state of single crystal can overcome the drawbacks of strong light scattering, low transmission and low chemical stability of that in state of nano-crystal[8,9]. The capability of generating white light is demonstrated from the combination of simultaneous emissions of blue (Dy^{3+}:$^4F_{9/2}\rightarrow{}^6H_{15/2}$), yellow ($Dy^{3+}$:$^4F_{9/2}\rightarrow{}^6H_{13/2}$), orange ($Eu^{3+}$:$^5D_0\rightarrow{}^7F_1$) and red ($Eu^{3+}$: $^5D_0\rightarrow{}^7F_2$) light waves[1,4,10,11] under the excitation of ultraviolet (UV) light.

From the phase diagram of NaY-YF_3 system[12], the cubic lattice $NaYF_4$ single crystal is difficult to be obtained from the melt of NaY-YF_3 directly due to the complex phase equilibrium. KF was found to be a critical assistant flux to grow cubic lattice $NaYF_4$ single crystal from the melt of NaY-YF_3 system. NaF, YF_3, DyF_3, EuF_3 and KF powders with high purity of 99.99% were used as raw materials with molar compositions of 30NaF-18KF-52YF_3, 30NaF-18KF-51YF_3-1DyF_3 and 30NaF-18KF-51YF_3-0.8DyF_3-0.2EuF_3 for undoped, sin-

* This work has been supported by the National Natural Science Foundation of China (Nos.51472125 and 51272109), and the K. C. Wong Magna Fund in Ningbo University.

** E-mail: hpxcm@nbu.edu.cn

gly- and co-doped crystal samples, respectively. The weighed mixture of those materials was ground for about 1 h in a mortar. The moisture and some oxygen impurities in the fluoride powders could be removed completely using the high temperature hydrofluorination method by which the powders were sintered under air of anhydrous HF at 750 °C for 8 h. The seed with *a*-axis was put in the bottom of seed well, and the sintered polycrystalline powders were filled in platinum crucibles with size of Φ10 mm×120 mm. The temperature gradient cross solid-liquid interface was 70–90 °C/cm. The growth process was carried out by lowering the crucible at a rate of ~0.6 mm/h. The detailed process is similar to the growth process of $LiYF_4$ single crystal reported in Ref.[13]. The single crystal was cut into pieces and well polished to ~2.0 mm thickness for optical measurement.

The Dy^{3+} or Eu^{3+} doping concentrations in cubic lattice $NaYF_4$ single crystals were measured by the inductive coupled plasma (ICP) atomic emission spectroscopy (PerkinElmer Inc., Optima 3000). The cubic lattice $NaYF_4$ single crystal co-doped with Dy^{3+}/Eu^{3+} ions (1.193%/0.211%) (designated DE0) was grown as the lower part in the initial stage, and that co-doped with Dy^{3+}/Eu^{3+} ions (1.205%/0.366%) (designated DE1) was grown as the upper part in the final stage. The cubic lattice $NaYF_4$ single crystal doped with Dy^{3+} ions (1.60%) (designated D0) was also grown for comparison. The X-ray diffraction (XRD) measurements for identifying the phase composition of the crystal were performed on an XD-98X diffractometer (XD-3, Beijing). The Cary 5000 UV/VIS/NIR spectrophotometer (Agilent Co., America) recorded the absorption spectra from 240 nm to 600 nm. The optical properties of the samples were characterized by excitation spectra and photoluminescence spectra measured by an F-4500 spectrophotometer (Hitachi high-technologies Co., Tokyo Japan). All the measurements were carried out at room temperature.

Fig.1 presents the phase diagram of the condensed NaF-YF_3 system. It can be seen from Fig.1 that the shadow region is composed of three phases of cubic lattice $NaYF_4$, $NaY_{1.8}F_{6.4}$ and liquid. Due to the co-existence of multiple solid phases, it becomes extremely difficult to grow the cubic lattice $NaYF_4$ single crystal from melt of NaF-YF_3 system in shadow region and other phase regions directly. The fluoride salt KF, which has similar chemical characteristics to NaF, can be considered to be a proper flux to help the growth of cubic lattice $NaYF_4$. The introduction of KF changes the phase equilibrium between NaF and YF_3 completely and decreases the melting point of cubic lattice $NaYF_4$, which results in the crystallization of cubic lattice $NaYF_4$ only from the mixture when it is cooled. The raw materials with proper chemical molar compositions of 30% NaF-18% KF-52% YF_3 were determined after a lot of growing experiments.

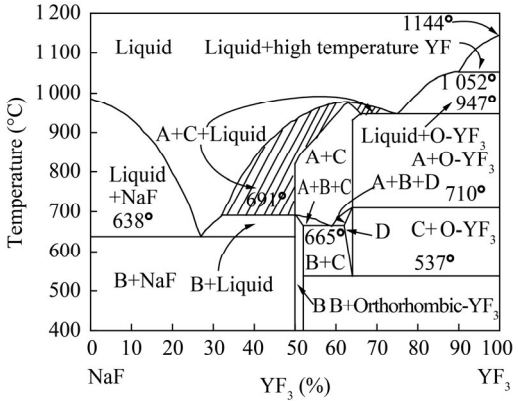

Fig.1 The phase diagram of the condensed NaF-YF_3 system in which cubic lattice $NaYF_4$, hexagonal $NaYF_4$, $NaY_{1.8}F_{6.4}$, ordered $NaY_{1.8}F_{6.4}$ are labeled as A, B, C and D, respectively

Fig.2 displays the XRD patterns of the Dy^{3+}/Eu^{3+} co-doped single crystals located at upper, middle and lower parts, as well as the reference card (JCPD # 77-2042) of cubic lattice $NaYF_4$, which are labeled as (a), (b), (c) and (d), respectively. Fig.2(e) shows the boule of the obtained transparent cubic lattice $NaYF_4$ single crystal. To better understand the phase composition of the obtained single crystal, the corresponding lattice plane indexes are marked in Fig.2(d). It can be easily found that the positions of diffraction peaks for middle and lower parts all well correspond to those of standard cubic lattice $NaYF_4$ (JCPD # 77-2042), while the upper part shows that the dominant cubic lattice $NaYF_4$ phases and a little other phases mainly consist of hexagonal $NaYF_4$, KYF_4, etc. It proves that the addition of flux KF does not have a large impact on the main cubic lattice $NaYF_4$ phase of transparent crystal structure. In this experiment, the crystal is co-doped with Dy^{3+}/Eu^{3+} ions. Thus, the XRD patterns also suggest that the current doping level does not cause any meaningful effect on cubic lattice $NaYF_4$ single crystal structure. As is well known, the cubic lattice $NaYF_4$ single crystal has fluorite structure (CaF_2), in which Na^+ and Y^{3+} ions are randomly distributed in the cation sites where are situated in cubic center, and according to the XRD pattern data, its lattice parameters can be calculated as $a_L=b_L=c_L=0.564\ 0$ nm, $a_M=b_M=c_M=0.567\ 2$ nm and $a_U=b_U=c_U=0.584\ 0$ nm for lower, middle, and upper parts of crystal, respectively.

Fig.3 exhibits the absorption spectra of the samples DE0, D0 and undoped cubic lattice $NaYF_4$ single crystal ranging from 240 nm to 600 nm. It is evident that the undoped cubic lattice $NaYF_4$ single crystal has no visible absorption peak, while the absorption spectrum of D0 crystal shows the unique absorption peaks located at about 325 nm, 348 nm, 364 nm, 387 nm and 452 nm, which are ascribed to Dy^{3+} transitions from the $^6H_{15/2}$ ground state to higher states ($^6P_{3/2}$, $^4M_{17/2}$), ($^6P_{7/2}$, $^4I_{11/2}$), ($^6P_{5/2}$, $^4P_{3/2}$), ($^4I_{13/2}$,$^4F_{7/2}$) and $^4I_{15/2}$, respectively. Comparing the absorption spectrum of DE0 with that of D0,

there are some slight differences in not only the absorption peak intensity but also additional peaks centered at about 318 nm and 394 nm ascribed to Eu^{3+} transitions from $^7F_0$ to higher states of $^5H_4$, $^5L_6$. Meantime, the absorption spectrum of DE0 also implies that cubic lattice $NaYF_4$ single crystals co-doped with Dy^{3+}/Eu^{3+} can be excited efficiently by UV light or blue light.

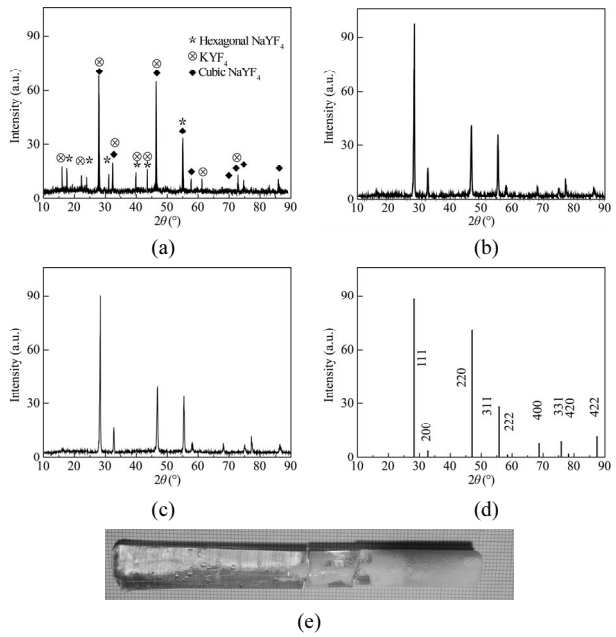

Fig.2 The XRD patterns of Dy^{3+}/Eu^{3+} co-doped single crystal located at (a) upper, (b) middle and (c) lower parts, as well as (d) the reference card (JCPD # 77-2042) of cubic lattice $NaYF_4$; (e) The boule of the obtained crystal

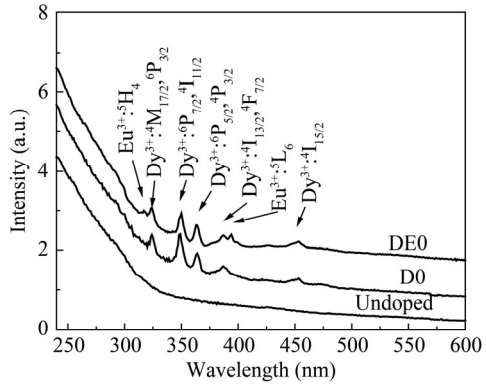

Fig.3 Absorption spectra of samples DE0, D0 and undoped cubic lattice $NaYF_4$ single crystal

Fig.4 displays the emission spectra of the samples D0 and DE0 under the 387 nm excitation. The emission spectra of both D0 and DE0 show a stronger blue emission band centered at ~479 nm corresponding to the magnetic dipole transition (Dy^{3+}:$^4F_{9/2}\rightarrow{}^6H_{15/2}$), a yellow emission band centered at ~571 nm ascribed to the electric dipole transition (Dy^{3+}:$^4F_{9/2}\rightarrow{}^6H_{13/2}$), and a weaker red emission band centered at ~659 nm due to the Dy^{3+}:$^4F_{9/2}\rightarrow{}^6H_{11/2}$ transition. It can be noted that two additional emission peaks centered at ~590 nm, which have partly overlapped with Dy^{3+} characteristic band at ~571 nm and ~612 nm ascribed to the Eu^{3+} ions transition ($^5D_0\rightarrow{}^7F_J$) (J=1, 2), appear in the Dy^{3+}/Eu^{3+} co-doped sample DE0. The above results imply that the Dy^{3+}/Eu^{3+} co-doped cubic lattice $NaYF_4$ single crystals can emit blue, yellow and red light simultaneously under the UV excitation, which also can obtain a better white light emission for w-LED application.

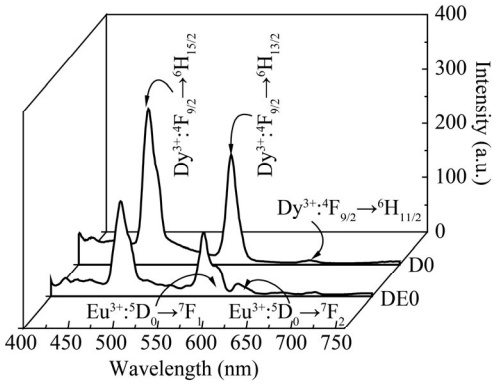

Fig.4 The emission spectra of the samples D0 and DE0 under 387 nm excitation

In order to obtain an optimal excitation wavelength, the excitation spectra of DE0 crystal are measured and displayed in Fig.5. The excitation spectra ranging from 300 nm to 400 nm are monitored by emissions at 479 nm, 571 nm and 612 nm, respectively. It can be seen from Fig.5 that the excitation spectrum monitored at 479 nm is very similar to that at 571 nm. Peaks centered at 324 nm (Dy^{3+}:$^6H_{15/2}\rightarrow{}^4M_{17/2}$, $^6P_{3/2}$), 348 nm (Dy^{3+}:$^6H_{15/2}\rightarrow{}^6P_{7/2}$, $^4I_{11/2}$), 364 nm (Dy^{3+}:$^6H_{15/2}\rightarrow{}^6P_{5/2}$, $^4P_{3/2}$) and 387 nm (Dy^{3+}: $^6H_{15/2}\rightarrow{}^4I_{13/2}$, $^4F_{7/2}$) are observed, respectively, and the luminescence intensities monitored by blue light emission at 479 nm are stronger than those monitored by yellow light at 571 nm when Dy^{3+}/Eu^{3+} co-doped crystal is excited by light ranging from 300 nm to 400 nm. However, there is only one visible peak located at 394 nm ascribed to $^7F_0\rightarrow{}^5L_6$ of Eu^{3+} referring to the spectrum monitored at 612 nm. As shown in Fig.5, the excitation wavelengths at 324 nm, 348 nm, 364 nm, 387 nm and 394 nm are selected as excitation wavelengths to achieve the optimized white light.

Figs.6 and 7 display the emission spectra of DE0 and DE1 samples under the excitation of 324 nm, 348 nm, 364 nm, 387 nm and 394 nm, respectively, which show the similar emission characteristics. When samples excited by various wavelengths, the emission spectra of cubic lattice $NaYF_4$ single crystal co-doped with Dy^{3+}/Eu^{3+} show a stronger blue emission, a moderate yellow emission and a weaker red emission, respectively. It becomes possible to obtain a better white light emission as a result of simultaneous blue, yellow and red light emitted from above samples under excitation of UV light.

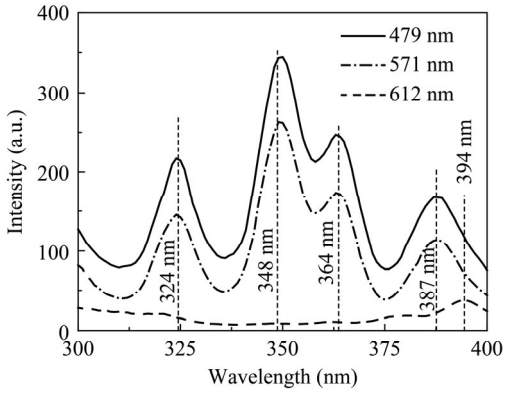

Fig.5 The excitation spectra of DE0 crystal monitored at 479 nm, 571 nm and 612 nm

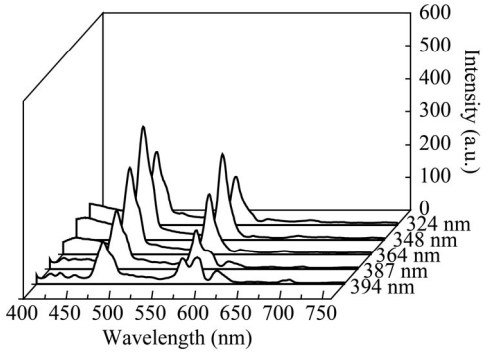

Fig.6 The emission spectra of DE0 sample under the excitation of 324 nm, 348 nm, 364 nm, 387 nm and 394 nm, respectively

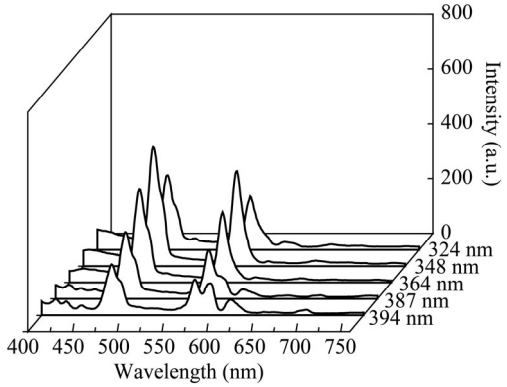

Fig.7 The emission spectra of DE1 crystal under the excitation of 324 nm, 348 nm, 364 nm, 387 nm and 394 nm, respectively

To analyze the real luminescence colors of the samples DE0 and DE1 under the excitation of 324 nm, 348 nm, 364 nm, 387 nm and 394 nm, the Commission Internationale de l'Eclairage (CIE) 1931 (x, y) chromaticity coordinates for those, which are necessary to be marked in the standard CIE chromaticity coordinate diagram, can be calculated according to the emission spectra by[14]

$$\begin{cases} x = X/(X+Y+Z) \\ y = Y/(X+Y+Z) \\ z = Z/(X+Y+Z) \end{cases}, \tag{1}$$

where X, Y and Z are three tristimulus values given by[14]

$$\begin{cases} X = \int_{\lambda} P(\lambda)\bar{x}(\lambda)\mathrm{d}\lambda \\ Y = \int_{\lambda} P(\lambda)\bar{y}(\lambda)\mathrm{d}\lambda \\ Z = \int_{\lambda} P(\lambda)\bar{z}(\lambda)\mathrm{d}\lambda \end{cases}, \tag{2}$$

where λ is the wavelength of the equivalent monochromatic light. $P(\lambda)$ is spectral power distribution, and its data are shown in Figs.6 and 7. $x(\lambda)$, $y(\lambda)$ and $z(\lambda)$ are the three color matching functions.

The correlated color temperature (T_c) is a key technical factor for evaluating warmer or cooler color appearance of a luminescence material. And it can be calculated by software of Chromaticity Coordinates To Color Temperature Conversion. We also know that the quantum efficiency is an important parameter for assessing the applicability of an optical material. But the quantum efficiency for our single crystal with full color emissions is hard to estimate from the traditional methods reported in Ref.[15]. In the introduction of this paper, it refers to the lower phonon energy (~360 cm^{-1}) of $NaYF_4$ single crystal, so we can believe that the internal quantum efficiencies for the emitting levels of Dy^{3+} and Eu^{3+} can be higher when the doping concentrations of rare earth ions are not too high. Therefore, the higher quantum efficiencies for Dy^{3+} and Eu^{3+} can be achieved by adjusting their doping concentrations.

The CIE 1931 (x, y) chromaticity coordinates and the correlated color temperatures for samples DE0 and DE1 under the excitation of 324 nm, 348 nm, 364 nm, 387 nm and 394 nm are calculated, listed and labeled in Figs.8 and 9. It is evident that the emissions of samples DE0 and DE1 under the excitation of UV wavelengths all fall into the white light region. To further assess the luminescence performance of the light source, the color rendering index (R_a), and the color quality scale (Q_a) are introduced, and the detailed procedures for the calculations of R_a and Q_a are available in Refs.[16] and [17]. The brief calculations for these are provided as

$$R_a = \frac{\sum_{i=1}^{8}\left(100 - 4.6\Delta E_i\right)}{8}, \tag{3}$$

$$Q_a = 10\ln\left\{\exp\left[(100 - 3.1\times\Delta E_{rms})/10\right] + 1\right\}, \tag{4}$$

where ΔE_i is the difference in color appearance for each sample illuminated by the test source and the reference illuminant which can be computed in CIE $W^*U^*V^*$ uniform color space, and ΔE_{rms} is the root mean square (rms) of the 15 color differences for each sample illuminated by the test source and the reference illuminant. Note that Q_a can be calculated by Eq.(4) when the correlated color temperature of the test light source is above 3 500 K.

Those parameters of DE0 and DE1 crystals under the

394 nm excitation are calculated as R_{a0}=76, Q_{a0}=76 and R_{a1}= 78, Q_{a1}=76. From Figs.8 and 9 we can also find that the emission of crystals under the 394 nm excitation is much closer to the standard equal energy white light illumination (x=0.333, y=0.333). It indicates that Dy^{3+}/Eu^{3+} co-doped $NaYF_4$ single crystal can achieve a good white light emission when it is combined with commercial near UV chips (390 nm±5 nm). Although the white light emission can be achieved, more effort should be paid to decrease the color temperature and increase the color rendering index or the color quality scale of cubic lattice $NaYF_4$ single crystals co-doped with Dy^{3+}/Eu^{3+} ions, which is relegated to further works.

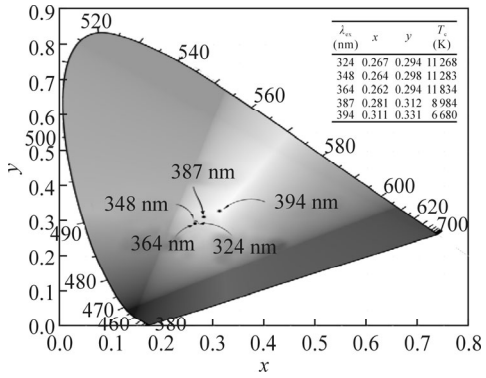

Fig.8 CIE chromaticity coordinates for DE0 sample under various excitation wavelengths

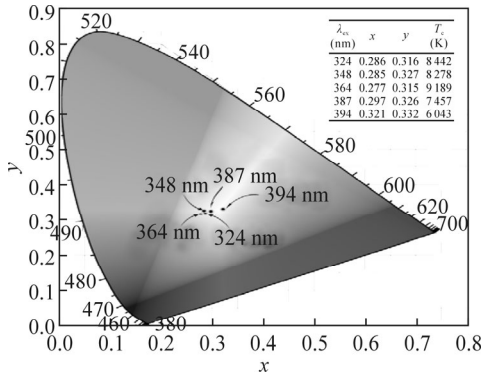

Fig.9 CIE chromaticity coordinates for DE1 sample under various excitation wavelengths

As a whole, the KF is found to be a very favorable assistant flux to grow cubic lattice $NaYF_4$ single crystal in $NaY\text{-}YF_3$ system, and the Dy^{3+}/Eu^{3+} co-doped cubic lattice $NaYF_4$ single crystal can be synthesized by a modified Bridgman method. Strong blue emission at ~479 nm, moderate yellow emission at ~571 nm and weak red emission at ~612 nm can be obtained simultaneously under excitation of UV light. A white light emission from the combination of the above three light waves with chromaticity coordinates of x=0.321, y=0.332, correlated color temperature of T_c=6 043 K, color rendering index of R_a=78 and color quality scale of Q_a=76 can be obtained from Dy^{3+}/Eu^{3+} co-doped cubic lattice $NaYF_4$ single crystal with doping molar concentrations of 1.205%/0.366% when excited by 394 nm light. Due to the chemical stability, high luminous efficiency and unique white light-emitting of Dy^{3+}/Eu^{3+} co-doped cubic lattice $NaYF_4$ single crystal, it can be a potential candidate for white LED application.

References

[1] C. F. Zhu, S. Chausseden, S. J. Liu, Y. F. Zhang, A. Monteil, N. Gaumer and Y. Z. Yue, Journal of Alloys and Compounds **555**, 232 (2013).

[2] WANG Pei-yuan, XIA Hai-ping, PENG Jiang-tao, TANG Lei and HU Hao-yang, Journal of Optoelectronics·Laser **24**, 2143 (2013). (in Chinese)

[3] DONG Yan-ming, XIA Hai-ping, FU Li, LI Shan-shan, GU Xue-mei, ZHANG Jian-li, WANG Dong-jie, ZHANG Yue-pin, JIANG Hao-chuan and CHEN Bao-jiu, Optoelectronics Letters **10**, 262 (2014).

[4] L. Fu, H. P. Xia, Y. M. Dong, S. S. Li, X. M. Gu, H. C. Jiang and B. J. Chen, IEEE Photonics Technology Letters **26**, 1485 (2014).

[5] Z. W. Jiao, S. X. Li, Q. F. Yan, X. Q. Wang and D. Z. Shen, Journal of Physics and Chemistry of Solids **72**, 252 (2011).

[6] J. F. Suyver, J. Grimm, M. K. van Veen, D. Biner, K. W. Krämer and H. U. Güdel, Journal of Luminescence **117**, 1 (2006).

[7] L. Gomes, A. F. H. Librantz, F. H. Jagosich, W. A. L. Alves, I. M. Ranieri and S. L. Baldochi, Journal of Applied Physics **106**, 103508 (2009).

[8] P. Liu, G. H. Zhou, J. Zhang, S. Chen, Y. Yang and S. W. Wang, Journal of Luminescence **144**, 57 (2013).

[9] M. Y. Ding, J. H. Xi, S. L. Yin and Z. G. Ji, Superlattices and Microstructures **83**, 390 (2015).

[10] W. S. Souza, R. O. Domingues, L. A. Bueno, E. B. da Costa and A. S. Gouveia-Neto, Journal of Luminescence **144**, 87 (2013).

[11] GU Chang-Jiang, CHEN Xiang-ying, SUN Dun-lu, LUO Jian-qiao, CHEN Jia-kang, ZHANG Hui-li, ZHANG Qing-li and YIN Shao-tang, Journal of Optoelectronics·Laser **25**, 491 (2014). (in Chinese)

[12] R. E. Thoma, G. M. Hebert, H. Insley and C. F. Weaver, Inorganic Chemistry **2**, 1005 (1963).

[13] H. Y. Hu, H. P. Xia, J. X. Hu, P. Y. Wang, J. T. Peng, Y. P. Zhang, H. C. Jiang and B. J. Chen, Journal of Alloys and Compounds **573**, 187 (2013).

[14] R. J. Mortimer and T. S. Varley, Displays **32**, 35 (2011).

[15] Y. Zheng, B. J. Chen, H. Y. Zhong, J. S. Sun, L. H. Cheng and X. P. Li, Journal of the American Ceramic Society **94**, 1766 (2011).

[16] TAN Li, LIU Yu-ling and YU Fei-hong, Optical Instruments **26**, 41 (2004). (in Chinese)

[17] W. Davis and Y. Ohno, Optical Engineering **49**, 033602 (2010).